Structural-order effects in low-energy electron transmission spectra of condensed Ar, Kr, Xe, N_2, CO, and O_2

G. Bader
Département de Physique et de Mathématiques, Université de Moncton, Moncton, New Brunswick, Canada E1A 3E9

G. Perluzzo
Groupe C.R.M. en Sciences des Radiations, Département de Médecine Nucléaire et de Radiobiologie, Faculté de Médecine, Université de Sherbrooke, Sherbrooke, Québec, Canada J1H 5N4

L. G. Caron
Centre de Recherche en Physique du Solide et Département de Physique, Faculté des Sciences, Université de Sherbrooke, Sherbrooke, Québec, Canada J1K 2R1

L. Sanche
Groupe C.R.M. en Sciences des Radiations, Département de Médecine Nucléaire et de Radiobiologie, Faculté de Médecine, Université de Sherbrooke, Sherbrooke, Québec, Canada J1H 5N4
(Received 16 September 1983)

Low-energy electron transmission spectroscopy is sensitive to crystal order and electronic band structure. The latter is responsible for minima in transmitted current whenever the incident electron energy coincides with that of a band gap. We propose a quasi-free-electron model to describe the experimental results for Ar, Kr, Xe, N_2, CO, and O_2 films deposited on Pt. It contains two parameters: the energy of the bottom of the conduction band V_0 and an average electron effective mass m^*. The onset of inelastic processes is extremely valuable in determining V_0. Further knowledge of the reciprocal-lattice vectors allows a reliable fit to m^* and V_0. The results for Xe join smoothly to those of higher-energy low-energy electron diffraction experiments. We are also able to correlate the average atomic structure factor to the minima in the elastic mean free path of Xe.

I. INTRODUCTION

Structures observable in low-energy electron transmission (LEET) spectra of condensed films[1] may be broadly divided into two categories:[2] those which result from elastic interactions and the others which are produced by energy-loss processes. These latter usually form broad maxima in dc LEET spectra resulting from a convolution of inelastically scattered electron currents created by phonons, excitons, and band-to-band transitions.[2–5] It has repeatedly been indicated in recent years[2–6] that the features appearing in the elastic part of dc transmission curves are most probably related to the structural order of the films via the energy dependence of a structure factor. Our results in solid rare gases[4–6] provided strong evidence for this hypothesis and indicated the possibility of differentiating between energy-loss and elastic features. We observed the effect of structural disorder, both thermal and positional, on the LEET spectra of Xe films deposited on a cold metal substrate.[4–6] The most-ordered films exhibited spectra having strong structures in the energy range where inelastic processes are negligible. The amplitude of these features were very sensitive to disorder. Moreover, they appeared strongly amplified in the energy dependence of the electron elastic mean free path as deduced from a fit using the two-stream model of Bader *et al.*[4] It became clear that low-energy electron transmission spectroscopy (LEETS) is sensitive to structural effects of which the electronic band structure is an inescapable by-product. As a matter of fact, it is well known that the electron-reflection coefficient on a perfect crystal is strongly dependent on the electronic band structure.[7–11] For instance, the specular reflection shows maxima for incident electron directions and energies coincident with those of forbidden gaps in the crystal band structure.[7–12] The reason is simply that electrons cannot propagate in a band gap (there are no available conduction states). LEET spectra, however, are usually recorded with polycrystalline or amorphous films,[1] and the results cannot necessarily be directly interpreted in terms of single-crystal band structure.

The present results were obtained from rare gases, N_2, CO, and O_2, deposited on polycrystalline platinum. The films thus formed were polycrystalline as deduced from angular distribution measurements of backscattered electrons.[13,14] They presumably contained microcrystals of various sizes and orientations. The experiment should therefore show an average effect over all directions. The above arguments for vacuum-crystal reflection can also be carried over to intergrain scattering. Orientational mismatch between microcrystals also leads to scattering which is enhanced whenever the energy and orientation are coincident with a gap. The diffusive motion of the electron within the bulk of the film, which was proven in Ref. 4, coupled to random microcrystal orientations, also leads to orientational averaging effects within the bulk. We then expect maxima in both vacuum-film reflectivity and intergrain scattering whenever the energy of the in-

cident electron coincides with that of a band gap in any direction (averaging effect) of the Brillouin zone of the microcrystals' band structure. Increased scattering in the bulk is known to reduce transmission[4] because of the increased likelihood of backscattering to vacuum. Consequently, both vacuum-film and bulk conditions are conducive to minima in transmitted current when the incident electron energy happens to correspond with that of a band gap.

It is the purpose of this paper to establish a correlation between the minima in transmitted current and the band structure for two families of molecular solids, and thus provide the basis for a simple low-energy scattering theory on polycrystalline surfaces. We have chosen the rare gases Ar, Kr, and Xe and the molecular solids N_2, CO, O_2 which are particularly illustrative. The electron scattering mechanisms, the crystal structure, and the general behavior of LEET spectra are quite similar within each family. Our general objective is to provide a basic understanding of low-energy electron interactions with molecular solids. This comprehension is essential to obtain a clear picture of low-energy electron processes associated with high-energy radiation effects, and may help in interpreting results from spectroscopies (e.g., photoelectron and x-ray absorption near edge structures) involving low-energy electron scattering within the sample. Further developments of LEETS may eventually provide a simple *nondestructive method* to characterize ordered or disordered film growth; in particular, to identify and analyze layer-by-layer construction of epitaxial films or layered device structures.

The experiment is described in Sec. II and the results are given in Sec. III. In Sec. IV we correlate the minima in transmitted current to the band structure which is characterized by only two descriptive parameters: an energy for the bottom of the conduction band (V_0) and an averaged electron effective mass (m^*). Our results for Xe join extremely well with the higher-energy band-structure information obtained in low-energy electron diffraction (LEED).[8,9] Those for the bottom of the conduction band (i.e., V_0 values) are in excellent agreement with the values determined from photoelectron experiments[15–17] and from the thresholds of exciton creation which appear in the present LEET spectra. In Sec. V we make a critical examination of a simple intermicrocrystal scattering process in order to explain the elastic cross-section energy dependence in LEET spectra. We presume the Born approximation is true and try to relate the scattering cross sections to an averaged atomic structure factor.

II. EXPERIMENT

The apparatus consists of a high-resolution electron transmission spectrometer[18] of the type described by Sanche[3] and Bader *et al.*[4] The spectrometer is housed in an ion- and titanium-pumped ultrahigh-vacuum system reaching a base pressure of 5×10^{-11} Torr. The main components include a trochoidal monochromator, a pair of deflector plates, and a closed-cycle refrigerated cryostat of variable temperature (10–300 K). The magnetically collimated electrons leaving the monochromator are deflected by the plates and impinge on a film condensed on a metallic substrate attached to the cold end of the cryostat. The metal substrate (i.e., the electron collector) is electrically isolated from the cryostat by a sapphire sheet. The current traversing the film is measured as a function of electron energy. The trochoidal monochromator has been previously described in detail.[19] In the present experiment the incident current is $\sim3\times10^{-9}$ A and the resolution is 0.04-eV full width at half maximum (FWHM) as measured by retarding potential analysis in vacuum. Similar measurements on W(100) give a FWHM of 0.07 eV.[4]

The films were grown on a polycrystalline platinum sheet. Before condensing our gases, the metallic substrate was either cleaned by resistive heating of 1500 K or by argon sputtering followed by annealing at high temperature. Both techniques gave the same transmission spectra. Matheson research-grade gases were used without further purification. They were admitted in the vacuum system through a tube located in front of the collector. Most of the molecules ($>98\%$) leaving the tube condensed on the cryostat. The actual number which deposited on the collector was estimated from geometrical considerations and gas kinetic theory (i.e., expansion of a known volume at a given pressure and temperature into vacuum,[3,20]) assuming a sticking coefficient of unity. The number of monolayers condensed on the collector could be estimated by calibrating the amount of gas injected to produce "one monolayer." Further details on this method are to be found in the recent work of Bader *et al.*[4] The temperature of the electron collector was maintained constant, controlled, and monitored by a thermocouple (Au—0.7 at.% Fe versus Chromel copper) secured to the copper block of the cryostat. We constantly monitored the position of the injection curve (i.e., the sharp rise near 0 eV in LEET spectra) to ensure that the films did not charge.

III. RESULTS

LEET spectra for Ar, Kr, and Xe are shown in Figs. 1(a)–1(c), respectively. Figures 2(a)–2(c) present those of N_2, CO, and O_2, respectively. The experimental conditions are outlined along with some data and results pertinent to the analysis. Apart from a decrease in energy scale in going from argon to xenon, the similarity in the general shape of the spectra of the rare-gas family is quite evident. This will be seen to be due to the size of the atoms. The case of the molecular crystals is not so obvious. The molecules have similar sizes and one might expect similar energy scales, but there is no clear correspondence between the spectra.

The LEET spectra can be divided into two energy regions. There is a low-energy region in which the electrons undergo quasielastic scattering with losses to low-energy vibrational and lattice modes. In the higher-energy part of the spectra, electronic inelastic processes are also occurring. The boundary between the two regions is determined by the onset of the first inelastic electronic excitation which, as previously discussed,[2–5] appears as a rapid rise in the transmitted current followed by a broad maximum. We determined the energy E_{it} of this inelastic threshold (see Fig. 3) by the intersection of the zero-current line with the tangent at the inflection point of the

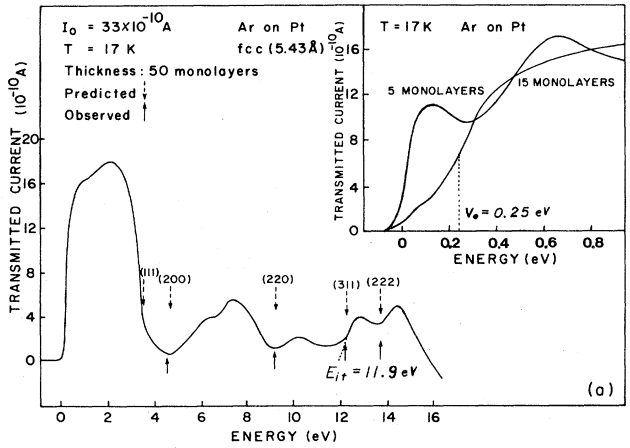

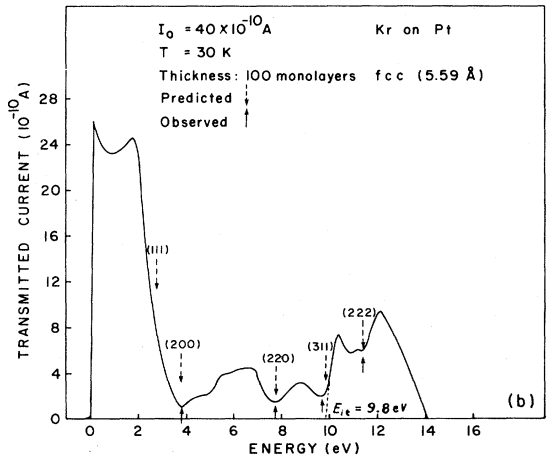

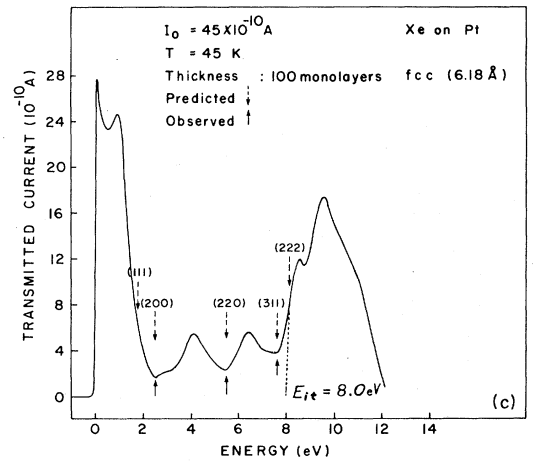

FIG. 1. Transmitted current plotted as a function of incident energy for rare-gas films. (See the text for the explanation of the arrows and the values of different parameters.)

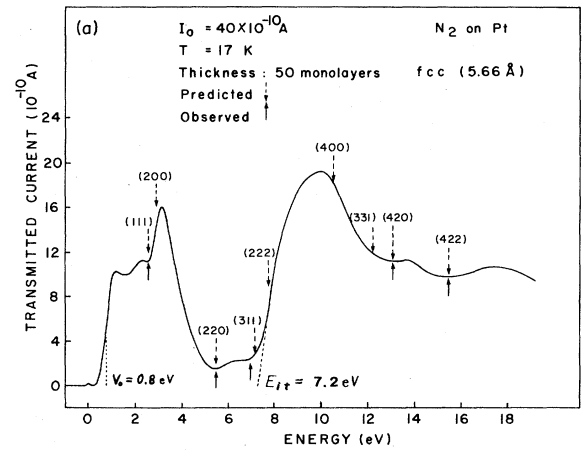

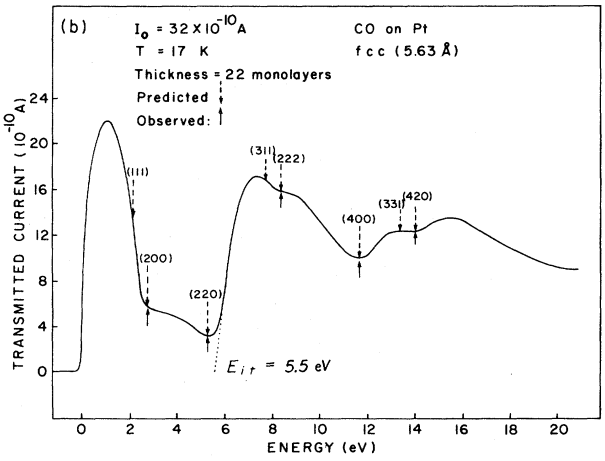

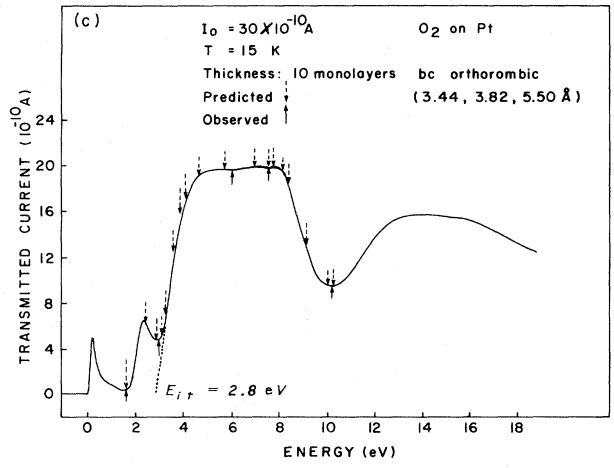

FIG. 2. Transmitted current vs incident electron energy for N_2, CO, and O_2 films. (See the text for the explanation of the arrows and the values of different parameters.)

rapid increase in transmitted current. The values are indicated in Figs. 1 and 2. The difference between E_{it} and the first exciton energy E_x is a good reference value for the energy at the bottom of the conduction band (V_0) of the film material (see Fig. 3). This is used in the next section to determine V_0 in CO, O_2, Kr, and Xe. In Ar and N_2, because V_0 is positive, its value can be measured directly. As shown in Figs. 1(a) and 2(a) V_0 is the energy at the maximum slope of the onset current for large film thicknesses.

IV. BAND-STRUCTURE EFFECTS

An obvious example of band-structure effects can be seen in the LEET spectra of N_2 and Ar which have a pos-

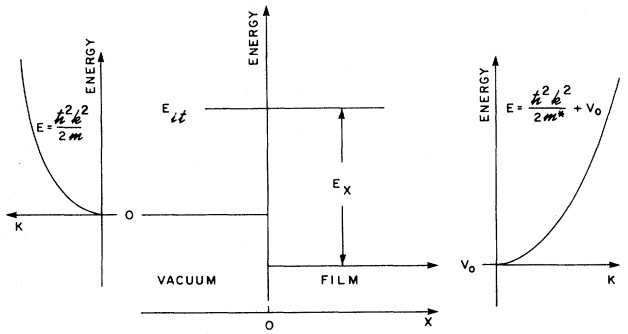

FIG. 3. Vacuum-film energy diagram showing the inelastic threshold conditions. When the incident electron reaches a threshold energy E_{it}, it can create an excitation of energy E_x, and falls to the bottom of the conduction band at energy V_0 (here negative). A parabolic conduction band with effective mass m^* is used in our model.

itive V_0. When the electron energy reaches 0.8 eV for N_2 [Fig. 2(a)] and 0.25 eV for Ar [insert Fig. 1(a)] the transmitted current rises sharply due to a sudden increase in the density of states (i.e., the beginning of the "quasi-free" electron conduction band). Note that we have taken the energy of maximum slope of the sharp current onset of the thickest samples as the most representative value of V_0. The zero of energy can be determined from measurements at small thicknesses where electrons can still traverse the film even in the band gap below V_0 [e.g., see insert Fig. 1(a)]. As discussed in the Introduction, we expect a directional averaging effect due to various microcrystal orientations which would bring out a minimum in transmission at every band-gap energy. This can be explained physically with the following arguments. As an electron reaches an interface between two microcrystals or between vacuum and a microcrystal, it will be reflected due to mismatches, to a greater extent if there is a gap at its energy and for its specific direction. Consequently, due to orientational averaging of microcrystals, we expect the specular reflection and the bulk elastic scattering cross section to have a maximum whenever the incident electron energy is coincident with that of a band gap (in any direction of momentum space). The band gaps in momentum space are located around the wave vectors which undergo optimal Bragg scattering,

$$\vec{K}=\tfrac{1}{2}\vec{G}\,, \tag{1}$$

where $\vec{G}$ is a reciprocal-lattice vector. If we further assume that electrons are quasifree, they can be reasonably well described by an effective mass m^* and an energy V_0 for the bottom of the paraboliclike conduction band (see Fig. 3). Thus we can write

$$E_G=\hbar^2(\tfrac{1}{2}G)^2/(2m^*)+V_0 \tag{2}$$

as an approximate relationship giving the energies E_G at which we expect band-gap effects to occur. This type of relationship is used in the higher-energy LEED experiment.[7–9] Although Eq. (2) seems a bit naive, it will be shown to be sufficient to explain our data. Our task is to correlate Eq. (2) to the experimental data. For each substance, we have selected representative minima in transmission spectra (indicated by up arrows) which we try to fit to Eq. (2).

We note that above the threshold for electronic losses (i.e., approximately 11.9, 9.8, 8.0, 7.2, 5.5 eV and 2.8 eV for Ar, Kr, Xe, N_2, CO, and O_2, respectively) band-structure minima are superimposed on broad inelastic maxima arising from electronic losses and band-to-band transitions.[5] It is therefore more difficult to perceive interference minima in these regions. This is particularly apparent in the case of O_2, because of the small value of E_{it}.

Knowledge of the lattice data of each solid[8,21] (indicated in the figures) is sufficient to determine all of its G values. All samples, except O_2, crystallize in the face-centered-cubic (fcc) structure at low temperature. We have taken the body-centered (bc) orthorhombic structure for O_2 at 17 K. The G values for this structure are not too dissimilar to those of the fcc structure. They bunch up in similar positions (see Fig. 5). We have then plotted the energy of the chosen minima as a function of the G value which we had tentatively assigned to each. These are shown in Fig. 4 for Ar, Kr, and Xe, and in Fig. 5 for N_2, CO, and O_2. The analysis of the molecular crystals CO and O_2 relies heavily on comparison with the other members of the family and on the inelastic threshold. At threshold (E_{it}) the incident electron has sufficient energy

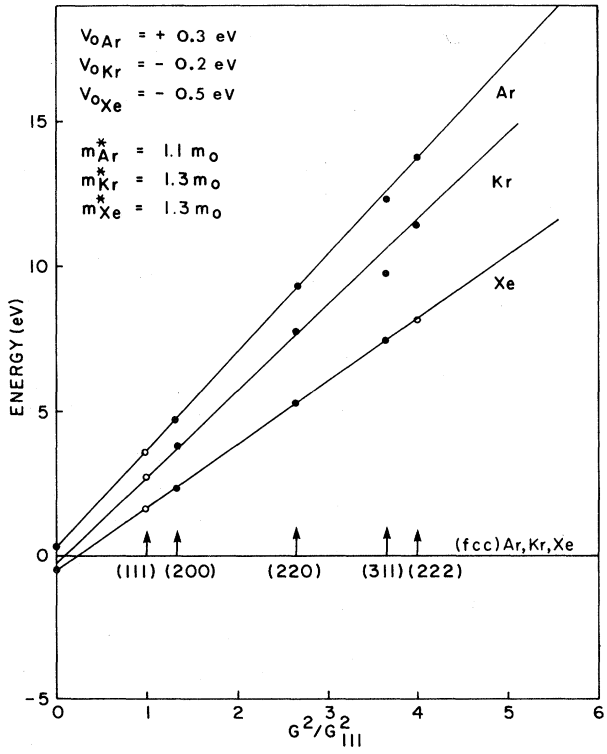

FIG. 4. The observed energy minima [solid circles corresponding to up arrows in Figs. 1(a)—1(c)] in the transmitted current are plotted versus G^2/G^2_{111} for the fcc structure of Ar, Kr, and Xe. (G is a reciprocal-lattice vector.) The open circles indicate unobserved minima in Fig. 1.

to create an excitation of energy E_x, such as band-to-band transition, and end up in a state at the bottom of the conduction band with energy V_0 (see Fig. 3), that is, for $E_{it}-V_0=E_x$. With a knowledge of E_{it} from LEETS and E_x from either electron energy-loss spectroscopy or optical data one can determine V_0 with fairly good accuracy. For example, in N_2 the inelastic threshold is at 7.2 eV while the value of V_0 is 0.8 eV. This implies in excitation energy of 6.4 eV, which agrees quite well with the first electronic transition found in gases [i.e., 6.3 eV (Ref. 22)]. For CO, using the known excitation energy to the first vibrational level of the $a^3\Pi$ state [6 eV (Ref. 22)] and the threshold value of 5.5 eV, we find $V_0\simeq 0.5$ eV. In the case of O_2, the inelastic threshold occurs at 2.8 eV while the onset of the Shumann-Runge continuum lies at 6.1 eV.[22] This leads to a value $V_0\simeq -3.3$ eV. Similarly, for rare gases the inelastic thresholds are 8, 9.8, and 11.9 eV for Xe, Kr, and Ar, respectively. The energy of the first excitons are 8.437, 10.033, and 11.624 eV for Xe, Kr, and Ar, respectively.[23] The V_0 values deduced are -0.5 eV for Xe, -0.2 eV for Kr, and $+0.3$ eV for Ar. They lie within 0.1 eV of those determined by other methods.[15–17]

We wish to emphasize the excellence of the fit of the data points by straight lines for all substances. The slopes, which set the energy scales of the spectra as discussed in Sec. III, are given by Eq. (2), that is, $\hbar^2G_{111}^2/(8m^*)$ for fcc [or $\hbar^2G_{011}^2/(8m^*)$ for bc orthorhombic] and allow us to deduce the effective masses m^*. The intercept with the vertical axis yields V_0. The results are shown in Figs. 4 and 5. All m^* values are quite acceptable and rather uniform within each family. For the rare gases, m^* being nearly the same, the energy scales of the LEET spectra are set by the slopes $\hbar^2G_{111}^2/(8m^*)$. Thus they are mostly dependent on G_{111}^2, which is in turn proportional to a_0^{-2}, where a_0 is the unit-cell lattice parameter. Larger atoms imply a larger a_0 and a smaller G_{111}^2. This leads to a more compact energy scale. This explains the comment on the correlation between the energy scales and the molecular size made in the preceding section. Furthermore, we can now use the fitted straight lines to deduce the expected occurrence (in energy) of all G vectors, that is, of expected band-gap effects in LEET spectra. We have shown some of these expected positions by down arrows in Figs. 1 and 2. Some expected minima are not visible, while some others are shifted as noted earlier. Inelastic collisions can drastically affect the shape of LEET spectra[1–5] and often mask the effect of elastic scattering responsible for the minima.

The band-effect minima can be better seen on a plot of the elastic mean free path (MFP) which is not cluttered by inelastic effects. This is the case for Xe where the fit has been made.[4] We will further discuss this point in the next section.

As an additional check on our effective-mass hypothesis, we have compared our low-energy results of Eq. (2) with the higher-energy data of Ignatiev *et al.*[8,9] This

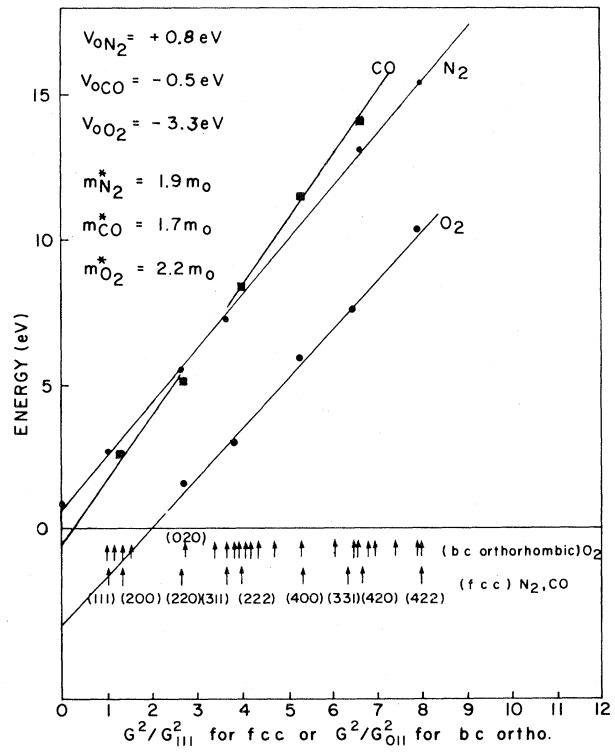

FIG. 5. The observed energy minima [indicated by upward arrows in Figs. 2(a)–2(c)] in the transmitted current are plotted versus G^2/G_{111}^2 for the fcc structure of N_2 and CO and versus G^2/G_{011}^2 for the bc orthorhombic structure of O_2 (G is a reciprocal-lattice vector).

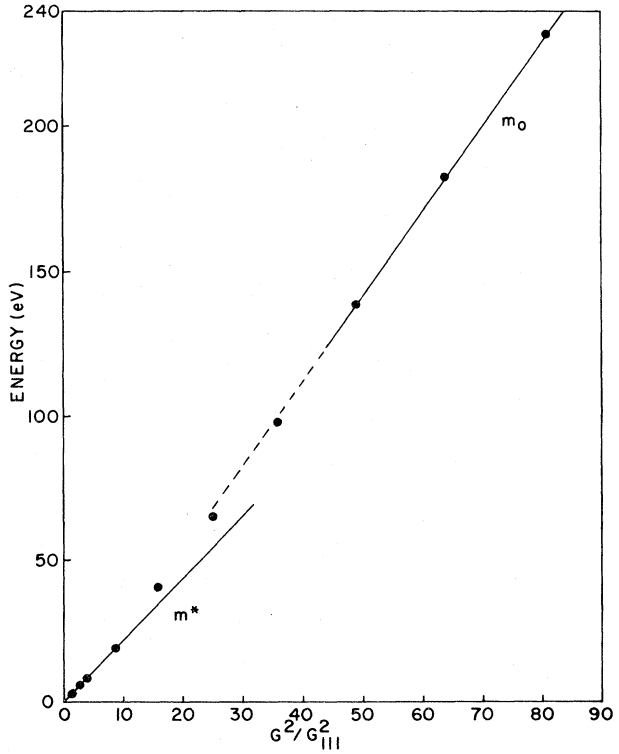

FIG. 6. Energy minima of Xe in the transmitted current plotted versus G^2/G_{111}^2. The parts about 15 eV are obtained by Ignatiev *et al.* (Ref. 9) as maxima in the (0,0) reflected beam as a function of energy (normal incidence) for a (111) oriented Xe crystal.

is shown in Fig. 6. The high-energy results of Ignatiev *et al.* clearly smoothly join with our results giving additional credence to our model. Note the difference in effective mass in the two energy regions. It is quite obvious by now that the effective-mass model is reliable in describing the band-structure effects in our samples. This effective mass is, of course, an average over all directions in momentum space.

V. STRUCTURE FACTOR

We shall attempt to link our model to a semiquantitative one by using the Born approximation for the scattering of an electron on a microcrystal in the case of Xe. One obtains an elastic differential cross section:[1,2,5,12,13]

$$\frac{d\sigma}{d\Omega}=\frac{d\sigma_0}{d\Omega}S(\vec{k}-\vec{k}'), \tag{3}$$

where $\vec{k}$ ($\vec{k}'$) are the incident (scattered) electron wave vectors and

$$S(\vec{k}-\vec{k}')=(2\Pi)^3 4a^{-3}\sum_{\vec{G}}\delta(\vec{k}-\vec{k}'-\vec{G}) . \tag{4}$$

$S(\vec{k}-\vec{k}')$ is the structure factor and $d\sigma_0/d\Omega$ is the differential cross section associated with a unit cell. Integrating this last equation over all $\Omega_{\vec{k}}$ and averaging over all $\Omega_{\vec{k}'}$, one obtains

$$\bar{\sigma}=\frac{1}{4\Pi}\int d\Omega_{\vec{k}}\int d\Omega_{\vec{k}'}\frac{d\sigma_0}{d\Omega}S(\vec{k}-\vec{k}') . \tag{5}$$

Assuming isotropic scattering for convenience,

$$\frac{d\sigma_0}{d\Omega}=\frac{\sigma_0(k)}{4\Pi} , \tag{6}$$

one finds

$$\bar{\sigma}=\sigma_0(k)\bar{S}(k) , \tag{7}$$

where

$$\bar{S}(k)=(4\Pi)^{-2}\int d\Omega_{\vec{k}}\int d\Omega_{\vec{k}'}S(\vec{k}-\vec{k}') . \tag{8}$$

We shall now try to see whether or not the observed data fit this type of behavior.

We examine the case of Xe for which we have already obtained the elastic MFP. It is inversely proportional to $\bar{\sigma}$. As discussed in the last section, the MFP of an ordered film shows minima at each predicted G value since the elastic MFP has extracted the information about elastic processes which are the only ones pertinent to this analysis. The first (111) minima is not visible on the published MFP curves but can be seen on extended scales. In order to eliminate the unknown $\sigma_0(k)$ we have taken the ratio of elastic MFP l_e for two different samples. It is thus assumed that $\sigma_0(k)$ is the same for the two samples. This is an approximation, since $\sigma_0(k)$ is surely sensitive to short-range order which is different for the two samples we have chosen. One sample was deposited at 15 K and is known to be disordered.[2–5] The other was deposited at 45 K and cooled to 15 K. It has the most ordered structure.[2–5] We then have

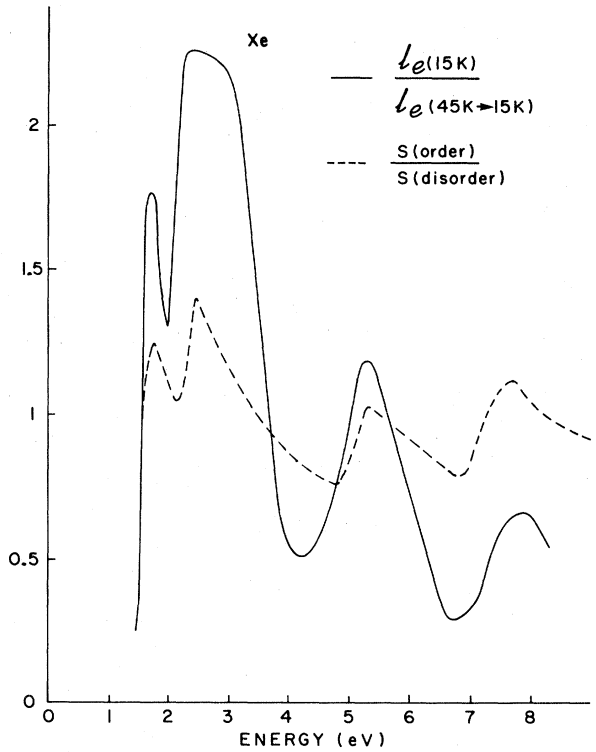

FIG. 7. The ratio of the mean free path of two different Xe films is plotted versus the incident energy and compared with the ratio of two averaged atomic structure factors (see text).

$$\frac{l_{e(15\text{ K})}}{l_{e(45\text{ K}\to15\text{ K})}}=\frac{\bar{\sigma}_{45\text{ K}\to15\text{ K}}(k)}{\bar{\sigma}_{15\text{ K}}(k)}\approx\frac{\bar{S}_{45\text{ K}\to15\text{ K}}(k)}{\bar{S}_{15\text{ K}}(k)} . \tag{9}$$

In order to simulate the effect of microcrystal size, we have used a Gaussian distribution for each vector in the reciprocal lattice in replacement of the delta function of Eq. (4). In Eq. (9) we converted the k dependence into an energy dependence by using the effective mass m^* and V_0 determined in the preceding section. We adjusted the widths of these Gaussians for each film (two parameters) to best reproduce the ratio of MFP. It has resulted that we must take a large width for the 15 K (which reduces $S_{15\text{ K}}$ almost to unity) and a very narrow width for the ordered $S_{45\text{ K}\to15\text{ K}}$. The result is shown in Fig. 7. The comparison is far from perfect (as can be expected from the rough approximations we made) but clearly shows the correct qualitative behavior about position, amplitude ratio, and widths of the structures. As was expected, the approximation of the structure factor is much too simple to reproduce the exact behavior of l_e but is sufficient to qualitatively explain the general behavior of the elastic MFP.

VI. CONCLUSION

It is well known that the intensity of the specular or of a given diffracted beam in LEED shows considerable structure as a function of electron-beam energy. This provides valuable information on the geometrical arrangement of the first few monolayers of a monocrystalline sur-

face. In the condition of the present experiment (i.e., 0—20 eV and normal incidence on the surface) the transmitted-current—versus—energy curves would be essentially complementary to the (0,0) intensity curves as long as inelastic effects are negligible and the sample film is well crystallized. In the case of polycrystalline films, however, intensity-versus-energy LEED measurements or LEET spectra can still exhibit considerable structures at low energies (0—20 eV), but these latter may not necessarily be explained by invoking single-crystal (0,0) beam intensities. Nevertheless, LEETS can provide useful information on the band structure in such polycrystalline films.

We have proposed a model in which the vacuum-film specular reflectivity and bulk grain boundary scattering show maxima at gap energies. These lead to minima in the transmitted current that can thus be correlated to the band structure. It should be noted, however, that bulk effects are not essential to the appearance of the minima. As a matter of fact, in cases where the microcrystals span the full thickness of the film and only azimuthal disorder exists, the (0,0) beam intensity at normal incidence does not see any disorder and there is little bulk influence (negligible intergrain scattering). Preliminary LEED calculations[24] under these conditions for Ar, Kr, and Xe seem to show structures which reproduce the gross features of our transmission experiments on polycrystalline samples. Thus structure due to specular reflection may well be an important factor in the LEET spectra of polycrystalline samples and probably a dominant one when only azimuthal disorder is present.

ACKNOWLEDGMENTS

The work of G. B. and L. G. C. was sponsored by the Natural Sciences and Engineering Research Council of Canada with further support from a special research fund to the University of Moncton for G. B. and Formation de Chercheurs et Action Concertée (FCAC) funds of the Québec Provincial Government for L. G. C. The work of G. P. and L. S. was sponsored by the Medical Research Council of Canada (MRCC) and Les Fonds de Recherche en Santé du Québec (FRSQ).

[1]For a review of the literature on low-energy (0—15 eV) electron total reflection and transmission experiments performed with solid films, see Ref. 2.
[2]L. Sanche, G. Bader, and L. G. Caron, J. Chem. Phys. **76**, 4016 (1982)
[3]L. Sanche, J. Chem. Phys. **71**, 4860 (1979).
[4]G. Bader, G. Perluzzo, L. G. Caron, and L. Sanche, Phys. Rev. B **26**, 6019 (1982).
[5]L. Sanche, G. Perluzzo, G. Bader, and L. G. Caron, J. Chem. Phys. **77**, 3285 (1982).
[6]G. Perluzzo, G. Bader, L. G. Caron, and L. Sanche, Phys. Rev. B **26**, 3976 (1982).
[7]J. B. Pendry, *Low Energy Electron Diffraction* (Academic, New York, 1979).
[8]A. Ignatiev, A. V. Jones, and T. N. Rhodin, Surf. Sci. **30**, 543 (1982).
[9]A. Ignatiev and T. N. Rhodin, Phys. Rev. B. **8**, 893 (1973).
[10]E. G. McRae, Surf. Sci. **25**, 491 (1971).
[11]G. Capart, Surf. Sci. **13**, 361 (1969).
[12]D. S. Boudreaux and V. Heine, Surf. Sci. **8**, 426 (1967).
[13]L. Sanche and M. Michaud, Phys. Rev. Lett. **47**, 1008 (1981), and results unpublished.
[14]L. Sanche and M. Michaud, Phys. Rev. B **27**, 3856 (1983); Chem. Phys. Lett. **84**, 497 (1981).
[15]N. Schwentner, M. Shibowski, and W. Steinmann, Phys. Rev. B **8**, 2965 (1973).
[16]N. Schwentner, F. J. Himpsel, V. Saile, M. Shibowski, W. Steinmann, and E. E. Koch, Phys. Rev. Lett. **34**, 528 (1975).
[17]N. Schwentner and E. E. Koch, Phys. Rev. B **14**, 4687 (1976).
[18]L. Sanche and G. J. Schulz, Phys. Rev. A **5**, 1672 (1972).
[19]A. Stamatovic and G. J. Schulz, Rev. Sci. Instrum. **41**, 423 (1970).
[20]T. E. Madey, Surf. Sci. **33**, 355 (1972).
[21]*Handbook at Chemistry and Physics,* 43rd ed., edited by D. D. Hodgman, R. C. Weast, and S. N. Selby (Chemical Rubber, Cleveland, 1961).
[22]G. Herzberg, *Spectra of Diatomic Molecules* (Van Nostrand, New York, 1950).
[23]L. Resca and S. Rodriguez, Phys. Rev. B **17**, 3334 (1978).
[24]C. Gaubert (private communication).